Chapter 2

Immunofluorescence of Microtubule Assemblies in Amphibian Oocytes and Early Embryos

Thao Nguyen, Timothy J. Mitchison, and Martin Wühr

Abstract

Amphibian oocytes and embryos are classical models to study cellular and developmental processes. For these studies, it is often advantageous to visualize protein organization. However, the large size and yolk distribution make imaging of deep structures in amphibian zygotes challenging. Here we describe in detail immunofluorescence (IF) protocols for imaging microtubule assemblies in early amphibian development. We developed these protocols to elucidate how the cell division machinery adapts to drastic changes in embryonic cell sizes. We describe how to image mitotic spindles, microtubule asters, chromosomes, and nuclei in whole-mount embryos, even when they are hundreds of micrometers removed from the embryo's surface. Though the described methods were optimized for microtubule assemblies, they have also proven useful for the visualization of other proteins.

Key words *Xenopus*, Amphibians, Immunofluorescence, Yolk clearing, Development, Embryos, Mitotic spindle, Microtubule asters, Large cells

1 Introduction

Amphibian oocytes and embryos are classical model systems to study cellular organization and vertebrate development. Swammerdam was probably the first person to describe cell division when he observed freshly laid frog eggs: "Next I observed the whole of the little frog divided, as it were, into two parts by an obvious fold or furrow" [1, 2]. A unique advantage of amphibian zygotes is their large size, which is on the order of 1 mm in diameter. This enables easy observation and manipulation. Hertwig and Pflueger deformed early frog embryos with glass plates and observed the reorientation of the cleavage plane leading to the famous Hertwig rule: the mitotic spindle cleaves the cell perpendicular to its longest axis [3, 4]. Currently *Xenopus laevis* is the predominant amphibian

Electronic Supplementary Material: The online version of this chapter (https://doi.org/10.1007/978-1-4939-9009-2_2) contains supplementary material, which is available to authorized users.

Francisco J. Pelegri (ed.), *Vertebrate Embryogenesis: Embryological, Cellular, and Genetic Methods*, Methods in Molecular Biology, vol. 1920, https://doi.org/10.1007/978-1-4939-9009-2_2,

model system for research. This is due to its year-round availability, easy in vitro fertilization, large embryos, rapid development, and ability to adapt to a wide range of laboratory conditions [5].

Besides their classical importance in studying vertebrate development, the introduction of *Xenopus* egg extract in the 1980s resulted in an important biochemical tool to study basic cell biology questions in a test tube [6–8]. *Xenopus* egg extract is essentially undiluted cytoplasm, which is considered "alive" by many accounts. Unlike more dilute forms of lysate, e.g., from tissue culture cells, the *Xenopus* egg extract can recapitulate many cellular processes in vitro. Among them are the formation of spindles, separation of sister chromatids, formation of nuclei, and recapitulation of cytokinesis as well as multiple rounds of cell cycles [9–12]. *Xenopus* egg extract has been a critical system to study spindle composition and formation, and has been more recently adapted to recapitulate millimeter-sized aster formation and aspects of cytokinesis in vitro [13–16]. More recently, *Xenopus* eggs, embryos, and lysates have become popular for quantitative proteomics experiments [17–20]. These systems are particularly attractive due to the large amount of material they provide at well-defined cellular or developmental stages. For example a single *Xenopus laevis* embryo contains ~30 μg of non-yolk protein [21].

Despite their utility in cell biological and developmental studies, amphibian eggs and embryos are difficult to image. This is due to their large size and widely dispersed yolk, rendering the embryos opaque. Nevertheless, visualizing oocytes and embryos is crucial for the interpretation of in vitro work and to connect molecular findings with underlying morphological changes. In the late nineteenth century Oskar Schultze performed pioneering work to image these structures deep inside the amphibian eggs and embryos. He visualized the meiotic spindle via thin-sectioning and some precursors of immunofluorescence (IF) [22] (Fig. 1a). However, whole-embryo imaging is hindered by yolk, which is dispersed throughout. Yolk contains crystalline proteins with higher density than cytoplasm. The light diffraction at the yolk-cytoplasm interface results in opaqueness of the embryo. Even with laser scanning microscopy live imaging is only possible close to the surface [23–25]. Kirschner and Murray proposed to replace the water in the embryos with a solution that matches the yolk's refractive index (~1.56 vs. ~1.33 of water). This solution is called "Murray's clear," consisting of a 2:1 mixture of benzyl benzoate and benzyl alcohol [26]. Murray's clear renders opaque eggs nearly transparent. Making use of this method, David Gard's lab pioneered the usage of laser scanning microscopy and IF in *Xenopus* embryos [27]. Here, we describe our adaptations of his lab's protocols for the imaging of microtubule structures in early development. We adapted these protocols to study how the cell machinery can find center and longest axes in cells that change their size within 5 h from a 1 mm single-cell

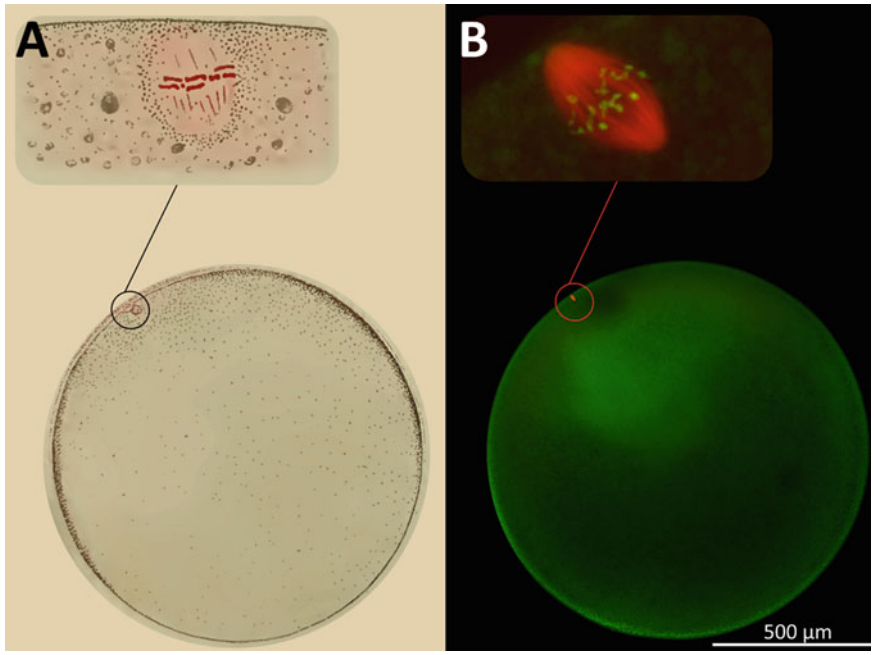

Fig. 1 Comparison of micrographs of the meiotic spindles in amphibians imaged in the nineteenth and twenty-first centuries. (**a**) Drawing of Schultze from 1887 based on observations of a meiotic spindle in the Axolotl egg obtained by thin sectioning and precursor to IF [22]. (**b**) Whole mount of a *Xenopus laevis* egg imaged with IF and laser scanning microscope based on protocols described in this chapter. Microtubules are shown in red, and DNA and unspecific background staining in green

fertilized egg to 25 µm cells at the midblastula transition [13, 14, 28, 29]. Our main modifications are as follows. First, we used a milder fixation condition that allows faster antibody penetration and deeper structure imaging even in whole-mount embryos. Furthermore, we reduced sample preparation time from ~1 week to ~3 days. We have primarily used this protocol to image specimens from *Xenopus laevis*. However, we also successfully adapted the protocol to obtain immunographs from Axolotl and *Xenopus tropicalis* [15]. An image of a whole-mount *Xenopus* egg with an observable meiotic spindle prepared using the protocol outlined here is shown in comparison with an immunograph of thin-sectioning meiotic egg visualized by Schultze in 1887 (Fig. 1).

2 Materials

2.1 Fixation

1. Methanol fixative: 90% Methanol, 10% 0.5 M EGTA pH 7.8 (adjust pH with KOH).
2. Low FG fixative (modified from [27]): 0.25% to 0.50% formaldehyde (from 37% stock), 0.1% glutaraldehyde (from 50% stock), 80 mM PIPES pH 6.8 (adjust pH with KOH), 1 mM $MgCl_2$, 5 mM EGTA, 0.2% Triton X-100.

3. 100% Methanol.
4. No. 5 watchmaker's forceps.
5. Scalpel.
6. Orbital shaker or nutator.

2.2 Rehydration

1. TBS: 10 mM Tris–HCl, pH 7.4, 155 mM NaCl (make as a 10× stock and add 0.65 g/L of NaN_3 to inhibit bacterial growth). Store at 4 °C.
2. 100% Methanol.
3. Orbital shaker or nutator.

2.3 Hemisecting

1. TBS.
2. Agarose cushion.
3. No. 5 watchmaker's forceps.
4. Scalpel.

2.4 Bleach

1. Bleach solution [30] (make fresh): 1% H_2O_2, 5% formamide, 150 mM NaCl, 16 mM sodium citrate, pH 7.0 (adjust pH with NaOH).
2. TBS.
3. Orbital shaker or nutator.

2.5 Stain

1. TBSNB [27] (make fresh): TBS, 0.1% Igepal CA-630, 1% BSA (prepare as a 10% stock and store at −20 °C), 2% fetal calf serum (FCS). Store at 4 °C for up to a week.
2. Tubulin labeling: Antibodies can be purchased pre-labeled (e.g., Alexa 488—Cat. # 322588, Thermo) or being labeled with dyes (e.g., APEX™ Antibody Labeling Kits, Invitrogen). We have successfully used Alexa 488, 547, or 647—longer wavelengths will result in less background fluorescence. Followings are some suggestions:
   (a) α-Tubulin monoclonal antibody (B-5-1-2) (T6074, Sigma)—for microtubules
   (b) γ-Tubulin monoclonal anti-γ-tubulin antibody (T5326, Sigma)—stains centrosomes
3. DNA staining: The chosen dye should be spectrally separable from the tubulin label:
   (a) TO-PRO-3 (far red) (Invitrogen)
   (b) YO-PRO-1 (green) (Invitrogen)
4. TBS.
5. Tin foil.
6. Orbital shaker or nutator.

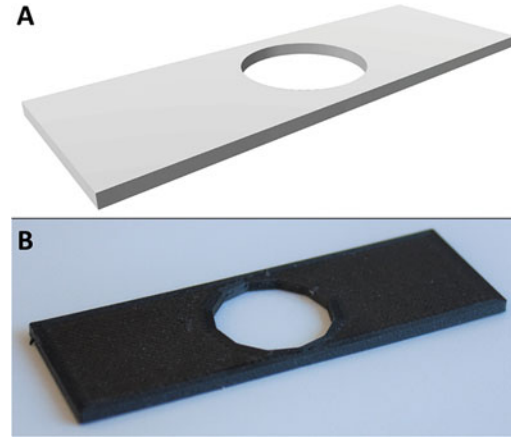

Fig. 2 A 3D printed mounting slide. (**a**) A 3D drawing of the mounting slide. (**b**) 3D printed Onyx (Markforged) slide, which is compatible with Murray's clear

2.6 Clear

1. Murray's clearing solution: 2:1 Benzyl benzoate:benzyl alcohol (BB:BA). Store at room temperature.
2. 100% Methanol.

2.7 Mount

1. Murray's clearing solution.
2. A 3D printed or machined cover slide with opening (Fig. 2 and *see* **Note 1**).
3. 25 mm Circle coverslips (No. 1.5, VWR).
4. Mini block heater (VWR) (*see* **Note 2**).
5. Confocal laser scanning microscope—e.g., LSM Zeiss 880.

3 Methods

We refer the readers to detailed protocols regarding collection of oocytes, eggs, testes, fertilization, and dejellying in previous publications [31–34].

3.1 Fixation

Fixation of the *Xenopus* embryo for IF microscopy requires a compromise between optimal preservation of cellular structures, antibody reactivity, and permeability of the antibody so that it can reach the target structures. Adapting from Becker and Gard [27], we recommend two different fixation conditions. The simpler and easier-to-reproduce procedure is the fixation with methanol with EGTA. The fix is performed at room temperature to prevent microtubule depolymerization. EGTA is added to capture Ca^{2+} ions, which might be released from the endoplasmic reticulum upon fixation and could lead to microtubule disassembly. The methanol fixation works well for metaphase and early anaphase/telophase microtubule. However, this soft fixation with methanol

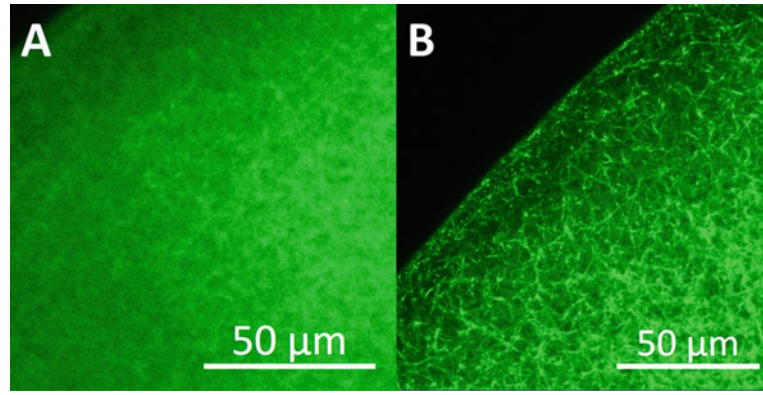

Fig. 3 Comparison of background microtubules (green) in the meiotic egg fixed with methanol or low FG. (**a**) Egg background microtubule organization in methanol fixation is poorly conserved. (**b**) The same microtubule network is clearly apparent with low FG fixation

often leads to deformed embryos. For instance, when samples are treated with methanol around the midblastula transition (MBT), the embryos often disassemble during sample handling. Lastly, some microtubules, e.g., the background network in the meiosis II egg, or late interphase/telophase asters, are only poorly preserved and hard to visualize with this fixation (Fig. 3a). We have obtained the best possible images with the low formaldehyde glutaraldehyde (low FG) fixation. Compared to the Gard protocol we omit the addition of the microtubule stabilizer paclitaxel. We were worried about the formation of new microtubules during the fixation process. With low FG fixation the background microtubules in the *Xenopus* egg can be nicely visualized (Fig. 3b). Furthermore, low FG-fixed embryos retain their shape better and stay intact even around the MBT. The disadvantage of this fix is that it requires more effort and results are harder to reproduce. Over-fixation can prevent deep antibody penetration. We therefore recommend cutting embryos with a scalpel every few minutes to check the progress while fixing. The embryos are fixed just right when the entire inside of the embryo is solid, and the entire cutting surface remains even. As soon as this is achieved, we transfer the embryos into MeOH/EGTA for postfixation of at least 24 h. Samples can be stored at 4 °C for months in methanol.

Methanol Fixation

1. Collect and submerge up to 20 dejellied embryos/eggs/oocytes in ~1.8 mL MeOH/EGTA solution in a 2 mL Eppendorf tube.
2. Gently flick the tube so that the specimen does not clump together.
3. Place the Eppendorf tube sideway on the shaker and leave it shaking gently at room temperature for at least 24 h. Continue to **step 6**.

Low FG Fixation

1. Collect and submerge 40 dejellied embryos/eggs/oocytes in low FG solution in a petri dish (*see* **Note 3**).
2. Place the dish on a shaker, gently shaking.
3. Check the eggs continuously (every few minutes) by cutting embryos with a scalpel in halves until they just turn solid.
4. The extent of proper fixation is rather specific in low FG method, e.g., too little then the microtubules are not preserved, or too much then the system becomes impenetrable to antibodies. The exact timing of low FG fixation can vary significantly depending on the (1) formaldehyde stock, (2) glutaraldehyde stock, and (3) exact fixation temperature.
5. Once the desired consistency is achieved, replace low FG solution with MeOH/EGTA for postfixation. Continue to **step 6**.

From this point onwards, both methods are the same:

6. Incubate the sample for at least 24 h in MeOH/EGTA while gently rotating on a nutator.
7. Replace the solution with 100% methanol.
8. STOP POINT store at 4 °C ad infinitum.

3.2 Rehydration

Antibodies are not methanol compatible. Prior to labeling, the sample needs to be rehydrated in a water-based solution. The rehydration process should be done gradually via multiple changes of TBS/MeOH solution with increasing TBS volume concentration to avoid bubble formation and disintegration of specimen. This is particularly important for methanol-fixed embryos.

1. Rehydrate embryos/eggs/oocytes in a sequence of 25%, 50%, 75%, and 100% TBS/methanol. Sample should be incubated in each solution for at least 30 min.
2. Store the samples in TBS.
3. SHORT-TERM STOP POINT.

3.3 Hemisecting Xenopus Oocytes and Eggs (Optional)

Hemisecting is useful because the large size of *Xenopus* oocytes, eggs, and embryos could hamper the penetration of antibodies—particularly after fixation with aldehyde. In addition, properly mounted hemisected oocytes and eggs allow visualization of regions of interest buried deep inside that would otherwise be inaccessible for short-working-distance objectives. When fixing later stage embryos with methanol, whole mount is highly recommended (*see* **Note 4**).

Routinely, we hemisect embryos/eggs/oocytes with a sharp scalpel prior to bleaching or staining; hence we retain the ability to tell the difference between the animal and vegetal poles (*see* **Note 5**).

1. Transfer the embryos to a petri dish with an agarose bed filled with buffer (100% TBS). The soft agarose bed helps to keep embryos intact during hemisecting.
2. Hemisect embryos along the desired axis with a scalpel.
3. After cutting, return oocytes to Eppendorf tubes filled with TBS.
4. SHORT-TERM STOP POINT.

3.4 Bleach Embryos

The pigments of *Xenopus* oocytes, eggs, and embryos attenuate laser illumination and obscure fluorescence. Pigmentation of fixed *Xenopus* oocytes can be eliminated by bleaching them with a solution of H_2O_2 (*see* **Notes 6** and **7**). Once bleached, the animal and vegetal hemispheres of the embryos/eggs/oocytes are often almost indistinguishable. If one works with albino embryos, this step is unnecessary (*see* **Note 8**).

1. Carefully aspirate the TBS.
2. To minimize accidental aspiration of samples, use a micropipette tip (preferably 200 μL) to reduce the bore of the Pasteur pipet tip.
3. Place the samples in the bleaching solution for a few hours or overnight. The required time varies depending on the number of samples in the bleaching solution and the amount of pigmentation. We suggest incubating the samples with the tubes on their sides on the shaker at room temperature (Fig. 4).
4. Carefully aspirate the bleaching solution.
5. Wash twice for ~15 min with TBS.
6. SHORT-TERM STOP POINT.

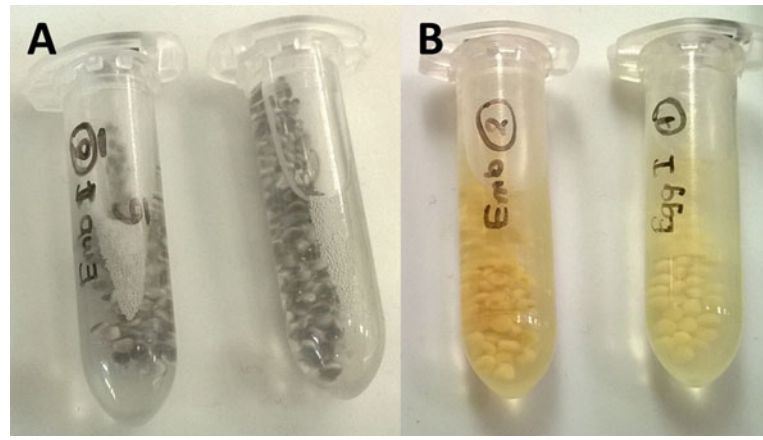

Fig. 4 Embryos before and after bleaching. (**a**) Post-rehydration, pre-bleaching embryos incubated in TBS. (**b**) Post-bleaching embryos incubated in TBS

3.5 Stain with Antibodies and DNA Dyes

Processing *Xenopus* embryos/eggs/oocytes for IF requires substantial antibody incubation time, with corresponding increase in the duration of intermediate washes, to allow the desired penetration (*see* **Note 9**). After staining, we dehydrate the prepared specimen with methanol to be able to transfer the embryos into the hydrophobic Murray's clear (*see* **Note 10**).

Multiple antibodies against cytoskeletal proteins with appropriate fixation conditions and working dilutions are listed in Table 1 in Becker and Gard's paper [27]. In this document, we only discuss antibodies against microtubules and dyes for DNA staining. We typically start with a 1:200 dilution of a 1 μg/μL antibody stock solution. The dilution can later be adjusted to either minimize background or increase brightness (*see* **Note 11**).

Here we exemplify the protocol with an Alexa-488-labeled α-tubulin antibody and the DNA dye TO-PRO-3 (*see* **Note 12**).

1. Submerge ~10 embryos in approximately 400 μL TBSNB.
2. Incubate primary labeled antibody (Alexa-488-labeled tubulin antibody) at 1:200 dilution (stock 1 μg/μL) in TBSNB.
3. Cover in tin foil and lay it down sideways on the shaker.
4. Incubate at 4 °C while gently shaking for at least 12 h (better 24 h).
5. Wash in TBSNB for at least 24 h (better 48 h) at 4 °C with a few times replacing buffer.
6. Keep the tube on gentle shaking mode and covered in tin foil.
7. Incubate in TBSNB for 30 min with TO-PRO-3 at 5 μM concentration.
8. Wash in TBSNB for 1 h.
9. Wash twice in TBS for 10 min.

3.6 Clear Embryos for Confocal Microscope

The yolk renders embryos/eggs/oocytes opaque and prevents visualization of structures no more than a few micrometers below the cell surface. The refractive index of Murray's clear closely matches that of yolk, thereby rendering *Xenopus* oocytes and eggs nearly transparent [26] (*see* **Note 13**).

1. Dehydrate samples in methanol in two changes.
2. Wash with MeOH for at least 15 min.
3. Repeat MeOH wash for 15 min for at least three times.
4. Aspirate the methanol.
5. Add ~1 mL Murray's clear to the samples. Allow them to clear and sink slowly to the bottom of the tube as they are infiltrated by Murray's clear solution (taking about 5–15 min). Do not stir the embryos in the solution.

6. When embryos have sunk, carefully remove the supernatant (Murray's clear mixed with methanol) and replace the top of vial with new Murray's clear (*see* **Note 14**).
7. At this point, the embryos should become transparent and somewhat difficult to identify in the solution (*see* **Note 15**).
8. SHORT-TERM STOP POINT (*see* **Note 16**).

3.7 Mount

Because of their size and physical properties, mounting *Xenopus* embryos/eggs/oocytes for high-resolution microscope poses some challenges. Therefore, they must be securely mounted between the coverslips to prevent movement during image collection period. We suggest orienting them so that the region of interest is at the closest proximity to the objective. Imaging with inverted microscopes is preferable. With upright microscopes the thickness of the mounting slide might need to be adjusted. For mounting whole oocyte/eggs/embryos, we suggest using double-sided chambers which have the dimensions of a typical glass and a thickness of 1.2 mm for whole mount or 0.8 mm for hemisected [27], with coverslips attached to both sides. For interested readers, we provide here (Supplementary Material) a 3D printable file of such a double-side chamber which is ready to use for a machine shop or common 3D printing vendors, e.g., https://www.3dhubs.com/. In our hands, Onyx (Fig. 2)—a 3D printable, filament made from nylon with micro-carbon reinforcement—works well, is cost effective, and is easy to obtain.

1. To make the mounting slide (Fig. 5), cut a small piece of parafilm (25 × 40 mm).
2. Place the parafilm beneath the mount; use a scalpel to go around the edge of the hole; cut out a circular piece. Discard the circular part and keep the cutout piece of parafilm.
3. Place the parafilm on top of the mount so that the circular hole and the chamber are aligned. Then place the coverslip on top of the parafilm.
4. Place the assembly on a heating block (~60 °C) for ~10 min with the coverslip facing downward. The heat will melt the parafilm to help glue the glass to the slide.
5. Once the parafilm melts, take the slide off the heating block. Gently push the glass against the mount to ensure sealing any gap. The mounting slide is ready for use.
6. Transfer the embryos (with the Murray's clear solution) onto the appropriate slide.
7. Add more Murray's clear solution until a convex meniscus forms (*see* **Note 17**).
8. Close the open side with a coverslip. Make sure that no air bubbles are trapped.

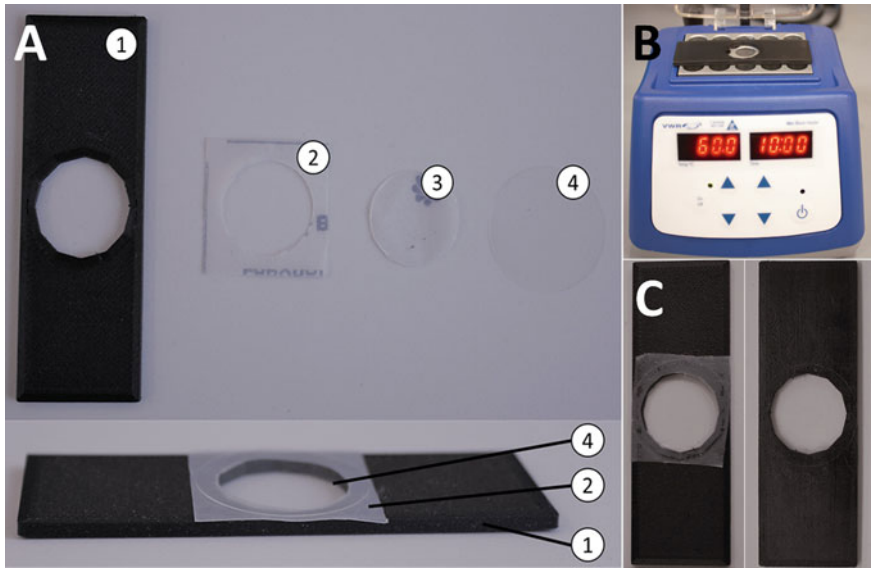

Fig. 5 Assembly of a mounting slide. (**a**) Components include (1) a mounting slide, (2) a cutout piece of parafilm, (3) a circular piece of parafilm—discard, and (4) a coverslip. The assembly is put together in the order from the bottom to the top: slide, parafilm, and coverslip. (**b**) Place the assembly with the coverslip facing downward on a heating block until the parafilm melts. (**c**) The result is a mounting slide with the bottom sealed by a coverslip

9. Gently press down on the coverslip to seat it properly.
10. Aspirate any excess Murray's clear expelled from the well.
11. Slides are immediately ready to view on the confocal microscope or storage for a few days in the dark at room temperature (*see* **Note 18**).
12. SHORT-TERM STORAGE.

How to optimally acquire laser scanning images has been extensively discussed elsewhere [35, 36]. In addition, postprocessing of confocal images is also discussed in detail in reference [37].

To demonstrate the versatility of the protocol we provide a few examples of *Xenopus* oocytes and embryos shown in Fig. 6. We believe for many IF experiments in amphibian systems, the outlined protocols are a useful starting point. A few previously published examples of IF imaging against, e.g., a mitotic regulator—AurkB, a mitotic kinesin—Kif20A, an actin-binding factor—Anln, and a cadherin-binding protein—Sept9 have successfully shown adaptability of these methods to other proteins [38, 39]. Please note that the difficult imaging conditions in amphibian oocytes and embryos might hinder visualization of low-abundant proteins. Some hints on whether imaging is possible can be obtained from proteomics studies with estimation of protein abundance in eggs and embryos [18, 40]. The proteins we were successfully able to image have estimated expression levels in the egg of at least 20 nM.

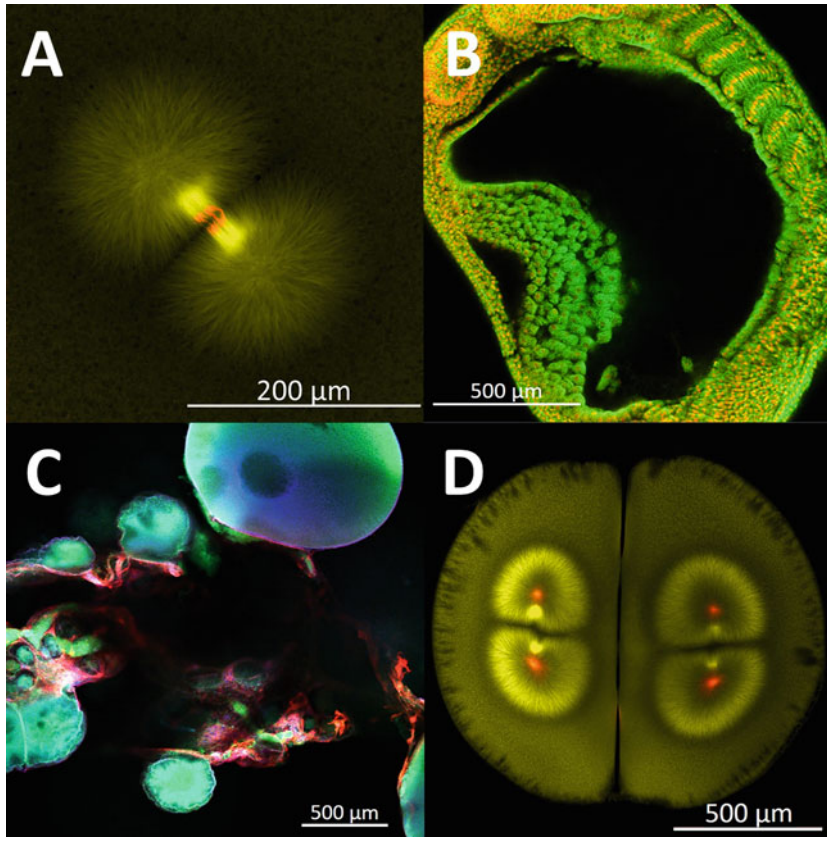

Fig. 6 Exemplary IF images of *Xenopus* oocytes and embryos. (**a**–**c** were fixed in methanol, and **d** in low FG.) (**a**) A close-up of the mitotic spindle in early anaphase from a one-cell-stage embryo. Chromosomes are shown in red, and microtubules in yellow. (**b**) An image of a methanol-fixed embryo at stages 32–34. Microtubules are shown in green, and DNA in red. (**c**) IF of a *Xenopus* ovary showing oocytes at various stages of growth. DNA and unspecific background is stained in green, microtubules are shown in blue, and intermediate filaments in red. (**d**) A two-cell embryo during anaphase/telophase. α-tubulin and γ-tubulin stainings are shown in yellow and red, respectively

4 Notes

1. A 3D model file is available in Supplementary Material.
2. Set heating block to ~60 °C.
3. We suggest to start with more specimens than needed because low FG fixation requires a few extra specimens for consistency check throughout fixation progress. We suggest using 2–3 specimens per inspection.
4. Hemisecting, however, may be unfavorable in later embryonic stages prior to gastrulation. At this point, embryos contain many cells that are loosely intact, and hemisecting increases their chance of falling apart.

5. We prefer to perform the cutting on an agarose cushion to hold the oocyte/egg/embryo in place, and to support the embryo leading to a cleaner cutting surface. Nevertheless, for simplicity, cutting directly on the plastic surface of a petri dish works reasonably well.
6. Perform the bleaching step prior to adding fluorophore to prevent bleaching of the fluorophore.
7. Peroxide bleach is very reactive with clothing and causes painful chemical burns on contact with skin. Gloves and protective glasses should be worn, and care taken when using bleach. In addition, be aware of whether the used antibodies/epitopes are compatible with peroxide bleach.
8. In an unbleached, non-albino embryo, animal hemisphere is pigmented while vegetal hemisphere is not. There is no easy procedure to distinguish the two hemispheres in a bleached or albino embryo.
9. To reduce time, we prefer to work with directly labeled primary antibodies. Directly labeled antibodies can be obtained commercially, or generated with amine-reactive dyes (e.g., APEX™ Antibody Labeling Kits, Invitrogen) [41]. In our experience, antibody incubation times of 12–24 h and washes of 24–48 h are satisfactory for either hemisected or whole-mount samples.
10. It is important to use dry methanol. If water is introduced into the clearing solution the specimen will not become fully transparent.
11. Diluted primary antibodies can be reused several times.
12. The most commonly used dyes for DNA such as Hoechst and DAPI are not compatible with Murray's clear. We have used TO-PRO-3 (far-red) and YO-PRO-1 (green) and observed good results for DNA staining of mitotic chromosomes. However, in our experience staining of nuclei in interphase is more finicky and harder to reproduce.
13. Murray's clear dissolves many plastics, including polystyrene and cellulose acetate [27]. Polypropylene tubes (e.g., Eppendorf tubes and some Falcon tubes) are resistant and should be used for all steps utilizing the clear. Finally, benzyl benzoate is an eye and skin irritant and should be handled with care.
14. The methanol-filled samples are lighter than Murray's clear; hence they are floating. Over time the methanol exchanges with Murray's clear and the samples will sink to the bottom. The methanol will stay close to the surface and can be easily removed.
15. If the samples remain cloudy still, they may not be completely dehydrated. Pass them through a few changes of methanol to

remove clearing solution and the remaining aqueous buffer; then re-clear with Murray's clear.

16. We observed that the sample might regain some opacity if stored in Murray's clear for too long.
17. At this point it might be advantageous to reorient the embryos as desired for imaging under a dissecting microscope.
18. Handle with care to keep the specimen in place.

Acknowledgments

We thank Sean Megason, Angela DePace, Evangelos Gatzogiannis, Mike Levine, and Laurence Lemaire for usage of their microscopes. Thanks to members of the Wühr Lab for comments on the manuscript. This work was supported by grants GM39565 and 1R35GM128813 from the National Institutes of Health and Princeton University startup funding.

References

1. Swammerdam J (1737) Bibilia Naturae; sive historia insectorum, in classes certas redact 2
2. Baker JR (1951) Remarks on the discovery of cell-division. Isis 42(130):285–287
3. Hertwig O (1893) Ueber den Werth der ersten Furchungszellen fuer die Organbildung des Embryo. Experimentelle Studien am Frosch- und Tritonei. Arch mikr Anat xlii:662–807
4. Pflüger E (1884) Ueber die Einwirkung der Schwerkraft und anderer Bedingungen auf die Richtung der Zelltheilung. Pflügers Arch Eur J Physiol 34(1):607–616. https://doi.org/10.1007/BF01612880
5. Wallingford JB, Liu KJ, Zheng Y (2010) Xenopus. Curr Biol 20(6):R263–R264. https://doi.org/10.1016/j.cub.2010.01.012
6. Lohka MJ, Maller JL (1985) Induction of nuclear envelope breakdown, chromosome condensation, and spindle formation in cell-free extracts. J Cell Biol 101(2):518–523
7. Sawin KE, Mitchison TJ (1991) Mitotic spindle assembly by two different pathways in vitro. J Cell Biol 112(5):925–940
8. Reinsch S, Karsenti E (1997) Movement of nuclei along microtubules in Xenopus egg extracts. Curr Biol 7(3):211–214
9. Lohka MJ, Masui Y (1983) Formation in vitro of sperm pronuclei and mitotic chromosomes induced by amphibian ooplasmic components. Science 220(4598):719–721
10. Coleman TR, Carpenter PB, Dunphy WG (1996) The Xenopus Cdc6 protein is essential for the initiation of a single round of DNA replication in cell-free extracts. Cell 87(1):53–63
11. Levy DL, Heald R (2010) Nuclear size is regulated by importin alpha and Ntf2 in Xenopus. Cell 143(2):288–298. https://doi.org/10.1016/j.cell.2010.09.012
12. Murray AW (1991) Cell cycle extracts. Methods Cell Biol 36:581–605
13. Wühr M, Dumont S, Groen AC, Needleman DJ, Mitchison TJ (2009) How does a millimeter-sized cell find its center. Cell Cycle 8(8):1115–1121
14. Wühr M, Chen Y, Dumont S, Groen AC, Needleman DJ, Salic A, Mitchison TJ (2008) Evidence for an upper limit to mitotic spindle length. Curr Biol 18(16):1256–1261. https://doi.org/10.1016/j.cub.2008.07.092
15. Mitchison T, Wühr M, Nguyen P, Ishihara K, Groen A, Field CM (2012) Growth, interaction, and positioning of microtubule asters in extremely large vertebrate embryo cells. Cytoskeleton (Hoboken) 69(10):738–750. https://doi.org/10.1002/cm.21050
16. Field CM, Pelletier JF, Mitchison TJ (2017) Xenopus extract approaches to studying microtubule organization and signaling in cytokinesis. Methods Cell Biol 137:395–435. https://doi.org/10.1016/bs.mcb.2016.04.014

17. Wühr M, Güttler T, Peshkin L, McAlister GC, Sonnett M, Ishihara K, Groen AC, Presler M, Erickson BK, Mitchison TJ, Kirschner MW, Gygi SP (2015) The nuclear proteome of a vertebrate. Curr Biol 25(20):2663–2671. https://doi.org/10.1016/j.cub.2015.08.047
18. Peshkin L, Wühr M, Pearl E, Haas W, Freeman RM Jr, Gerhart JC, Klein AM, Horb M, Gygi SP, Kirschner MW (2015) On the relationship of protein and mRNA dynamics in vertebrate embryonic development. Dev Cell 35 (3):383–394. https://doi.org/10.1016/j.devcel.2015.10.010
19. Lombard-Banek C, Moody SA, Nemes P (2016) High-sensitivity mass spectrometry for probing gene translation in single embryonic cells in the early frog (Xenopus) embryo. Front Cell Dev Biol 4:100. https://doi.org/10.3389/fcell.2016.00100
20. Smits AH, Lindeboom RG, Perino M, van Heeringen SJ, Veenstra GJ, Vermeulen M (2014) Global absolute quantification reveals tight regulation of protein expression in single Xenopus eggs. Nucleic Acids Res 42 (15):9880–9891. https://doi.org/10.1093/nar/gku661
21. Gurdon JB, Wickens MP (1983) The use of Xenopus oocytes for the expression of cloned genes. Methods Enzymol 101:370–386
22. Schultze O (1887) Untersuchungen uber die Reifung und Befruchtung des Amphibieneies. Erste Abhandlung. Z wiss Zool xlv:177–226
23. Kieserman EK, Lee C, Gray RS, Park TJ, Wallingford JB (2010) High-magnification in vivo imaging of Xenopus embryos for cell and developmental biology. Cold Spring Harb Protoc 2010(5):pdb prot5427. https://doi.org/10.1101/pdb.prot5427
24. Karasaki S (1963) Studies on amphibian yolk 1. The ultrastructure of the yolk platelet. J Cell Biol 18:135–151
25. Karasaki S (1963) Studies on amphibian yolk. 5. Electron microscopic observations on the utilization of yolk platelets during embryogenesis. J Ultrastruct Res 59:225–247
26. Dent JA, Polson AG, Klymkowsky MW (1989) A whole-mount immunocytochemical analysis of the expression of the intermediate filament protein vimentin in Xenopus. Development 105(1):61–74
27. Becker BE, Gard DL (2006) Visualization of the cytoskeleton in Xenopus oocytes and eggs by confocal immunofluorescence microscopy. Methods Mol Biol 322:69–86
28. Wühr M, Tan ES, Parker SK, Detrich HW 3rd, Mitchison TJ (2010) A model for cleavage plane determination in early amphibian and fish embryos. Curr Biol 20(22):2040–2045. https://doi.org/10.1016/j.cub.2010.10.024
29. Nieuwkoop PD, Faber J (1956) Normal table of Xenopus laevis (Daudin). A systematical and chronological survey of the development from the fertilized egg till the end of metamorphosis, vol 22. Garland Pub., New York, p 75
30. Mayor R, Morgan R, Sargent MG (1995) Induction of the prospective neural crest of Xenopus. Development 121(3):767–777
31. Vize P (2011) Inducing egg laying via hCG injection (Vize lab). http://wiki.xenbase.org/xenwiki/index.php/Inducing_egg_laying_via_hCG_injection_(Vize_lab)
32. VGP (2005) In vitro fertilization of Xenopus laevis (Conlon lab). http://wiki.xenbase.org/xenwiki/index.php/In_vitro_fertilization_of_Xenopus_laevis_(Conlon_lab)
33. VGP (2011) Dejellying embryos (Zorn lab). http://wiki.xenbase.org/xenwiki/index.php/Dejellying_embryos_(Zorn_lab)
34. Sive HL, Grainger RM, Harland RM (2007) Dejellying Xenopus laevis embryos. CSH Protoc 2007:pdb prot4731. https://doi.org/10.1101/pdb.prot4731
35. Paddock SW, Eliceiri KW (2014) Laser scanning confocal microscopy: history, applications, and related optical sectioning techniques. Methods Mol Biol 1075:9–47. https://doi.org/10.1007/978-1-60761-847-8_2
36. Ulrich M (2015) Confocal laser scanning microscopy. Hautarzt 66(7):504–510. https://doi.org/10.1007/s00105-015-3632-y
37. Gard DL (1999) Confocal microscopy and 3-D reconstruction of the cytoskeleton of Xenopus oocytes. Microsc Res Tech 44(6):388–414. https://doi.org/10.1002/(SICI)1097-0029(19990315)44:6<388::AID-JEMT2>3.0.CO;2-L
38. Nguyen PA, Groen AC, Loose M, Ishihara K, Wühr M, Field CM, Mitchison TJ (2014) Spatial organization of cytokinesis signaling reconstituted in a cell-free system. Science 346 (6206):244–247. https://doi.org/10.1126/science.1256773
39. Field CM, Groen AC, Nguyen PA, Mitchison TJ (2015) Spindle-to-cortex communication in cleaving, polyspermic Xenopus eggs. Mol

Biol Cell 26(20):3628–3640. https://doi.org/10.1091/mbc.E15-04-0233

40. Wühr M, Freeman RM Jr, Presler M, Horb ME, Peshkin L, Gygi SP, Kirschner MW (2014) Deep proteomics of the Xenopus laevis egg using an mRNA-derived reference database. Curr Biol 24(13):1467–1475. https://doi.org/10.1016/j.cub.2014.05.044
41. Groen AC, Mitchison TJ (2016) Purification and fluorescent labeling of tubulin from Xenopus laevis egg extracts. Methods Mol Biol 1413:35–45. https://doi.org/10.1007/978-1-4939-3542-0_3